must distort the medium, giving rise to a strain energy term. To evaluate the strain, the actual $\Delta l/l$ for the orienting species must be calculated.

Debye's Equation. Equation 18 is very similar to the Debye[9] equation. Furthermore, when the square brackets are taken to be unity, and g_r is set to 1, the Debye equation is obtained. However, the two differences just cited are quite important and in fact eliminate some of the original criticisms of the Debye theory. The one criticism is that short- and long-range correlations of the central dipole with its environment are neglected. In the present case the short- and long-range correlations are assumed to be structural rather than electrostatic in nature and are lumped into a geometric constant, g_r. The second criticism of the Debye equation is that it predicts an electrical Curie temperature. Equation 24 does not lead to an electrical Curie temperature for certain choices of the parameters. This point can be seen from the following variation of eq 18:

$$\frac{\epsilon_0 - 1}{\epsilon_0 + 2}\frac{3V}{4\pi} = N\left\{\frac{2D_0N}{6D_0NkT + Vg_r\gamma^2}\right\}g_r\mu^2 \qquad (22)$$

When $6D_0NkT < Vg_r\gamma^2$, eq 34 becomes

$$\frac{\epsilon_0 - 1}{\epsilon_0 + 2}\frac{3V}{4\pi} = \frac{2D_0N^2}{V}\frac{\mu^2}{\gamma^2} \qquad (23)$$

In other words, the polarizability, and hence the dielectric constant, are independent of temperature. Using the numerical constants in a previous section, the results are found to be quite reasonable and are given below:

For $D_0 = 10^{-6}$ dyn/cm^2

$$\frac{6D_0NkT}{Vg_r\gamma^2} = 2.49T$$

For $D_0 = 10^{-10}$ dyn/cm^2

$$\frac{6D_0NkT}{Vg_r\gamma^2} = 2.49 \times 10^{-4}T$$

In other words, for reasonably rigid systems with $\gamma \sim 2$, the polarizability, and hence ϵ_0, is independent of temperature.

References and Notes

(1) Mansfield, M. L. *J. Polym. Sci., Polym. Phys. Ed.* **1983**, *21* (5), 787.
(2) Perchak, D.; Skolnick, J.; Yaris, R. *Macromolecules* **1987**, *20*, 121.
(3) Onsager, L. *J. Am. Chem. Soc.* **1936**, *58*, 1486.
(4) Kirkwood, J. G. *J. Chem. Phys.* **1939**, *7*, 911.
(5) McCrum, N. G.; Read, B. E.; Williams, G. *Anelastic and Dielectric Effects in Polymeric Solids*; John Wiley & Sons: London, New York, and Sidney, 1967.
(6) Frohlich, H. *Theory of Dielectrics*; Clarendon Press: Oxford, England, 1949.
(7) Bottcher, C. J. F. *Theory of Electric Polarization*; Clarendon Press: Oxford, England, 1949.
(8) Timosenko, S.; Goodier, J. N. *Theory of Elasticity*; McGraw-Hill: New York, 1951.
(9) Debye, P. *Polar Molecules*; Dover Publications: New York, 1929.

Polydispersity Effects on Dilute-Solution Dynamic Properties of Linear Homopolymers

R. L. Sammler,† C. J. T. Landry,‡ G. R. Woltman, and J. L. Schrag*

Department of Chemistry and Rheology Research Center, University of Wisconsin, Madison, Wisconsin 53706.

Received October 10, 1989

ABSTRACT: The bead–spring model of Zimm is generalized to predict the effects of molecular weight polydispersity in samples of linear homopolymers. The predictions agree quantitatively with the frequency dependence of the modified birefringence coefficient, S^*_Δ, measured for several polydisperse samples ($1.06 < \bar{M}_w/\bar{M}_n < 2.5$) of atactic polystyrene dissolved in Aroclor 1248. At low levels of polydispersity the effects are only seen in the low-frequency transition zone; at higher levels the effects are seen at all frequencies. Estimations of the number-, weight-, and z-average molecular weights from the frequency dependence of the intrinsic birefringence are possible after calibration with monodisperse standards. Consideration of sample polydispersity (and approximating S_e with S'_∞) leads to a 15% reduction in past estimates of the molecular weight of a Gaussian submolecule for polystyrene dissolved in Aroclor 1248 at 25.00 °C. The similarity between the frequency dependence of S^*_Δ for a sample of linear chains with a bimodal molecular weight distribution and that for a monodisperse sample of regular combs underscores the need to assess sample polydispersity when using dynamic properties to interpret long-chain structure.

I. Introduction

The frequency dependences of the modified intrinsic birefringence, $[S^*]_\Delta$, and complex viscoelasticity, $[\eta^*]_\Delta$, coefficients have been shown[1] to have excellent potential for characterization of long-chain structure in monodisperse samples of flexible homopolymers. This potential is often best realized when data are obtained under good solvating conditions, and recent[2] computations have established the interpretation of Gaussian bead–spring model (BSM) fit parameters obtained by fitting such non-Θ properties. Real samples of homopolymers are sel-

† Current address: M. E. Pruitt Research Center, Dow Chemical Co., Midland, MI 48674.
‡ Current address: Corporate Research Laboratories, Eastman Kodak Co., Rochester, NY 14650.

0024-9297/90/2223-2388$02.50/0

dom monodisperse, and sample polydispersity is a potential complication in the analysis of long-chain structure. There are many types of sample polydispersity, and our interest here is restricted to molecular weight polydispersity in linear homopolymers and the effects it has on dynamic mechanical and optical properties. This work parallels that of Lovell and Ferry[3] who generalized the BSM of Zimm[4] to predict polydispersity effects on the storage, $[G']_R$, and loss, $[G'']_R$, components of the reduced intrinsic dynamic shear modulus; however, they made computational approximations, which restricted their application to low-frequency properties of infinitely long chains at the free-draining or non-free-draining limits. In contrast, here polydispersity effects are investigated in terms of the magnitude, $[S_{M\Delta}]$, and angle, $[\Theta_\Delta]$, components of the modified intrinsic birefringence coefficient (or their respective viscoelastic analogues, $[\eta_{M\Delta}]$ and $[\Phi_\Delta]$) because of their superior potential to characterize long-chain structure. More importantly, the predicted properties of these idealized samples are computed exactly with no restrictions on shearing frequency, chain size, or degree of hydrodynamic interaction. Hence, these are the first computations that enable polydispersity effects to be quantitatively investigated for samples with $\bar{M}_w$ below about 10^6, for polymer/solvent systems with any degree of hydrodynamic interaction and for properties measured at all but the highest shearing frequencies. The feasibility of these exact computations is a result of recent advances[5,6] that substantially reduce the labor in computing BSM properties for monodisperse samples of linear chains. Resultant predictions are quantitatively compared to the measured frequency dependence of $[S^*]_\Delta$ for atactic polystyrene samples dissolved in Aroclor 1248 (a polychlorinated biphenyl solvent). Samples with narrow ($\bar{M}_w/\bar{M}_n < 1.1$) and broad ($\bar{M}_w/\bar{M}_n \simeq 2.5$) polydispersities are studied. All data have been acquired with updated[7-11] instrumentation that now has sufficient sensitivity and precision to obtain infinite-dilution properties for at least six decades of reduced frequency (reduction with time–temperature superposition).

II. Prediction of Polydispersity Effects

Linear viscoelastic (VE) and oscillatory flow birefringence (OFB) properties are modeled for a polydisperse sample of linear homopolymers in dilute solution ($c[\eta] \ll 2$) when subjected to a low-shear-rate homogeneous shear flow. As usual, the homopolymer is also assumed to be flexible and amorphous and to have a uniform microstructure (e.g., tacticity, arrangement of head-to-head, tail-to-tail, or head-to-tail structures in vinyl polymers, level of geometric isomers or stereoisomers within the "repeat unit", etc.) so that long-chain structural features dominate the dynamic properties. The properties of each individual chain in the polydisperse sample are computed with a generalized form of the BSM of Zimm.[4] This well-known model represents a linear homopolymer as a chain of identical beads (radius a, mass m, friction coefficient ζ) connected by identical springs (Hookean force constant H); it also uses the "preaveraging" treatment of hydrodynamic interaction, employs Gaussian statistics, and ignores interchain interactions and inertial effects. The dilute-solution contribution of a chain composed of N springs to the complex mechanooptic coefficient, S^*, or the complex viscosity coefficient, η^*, is predicted to be

$$S^*_N \equiv S^* - S_e = q' n_N b^2 \sum_p \frac{\tau_{p,N}}{1 + i\omega\tau_{p,N}} \tag{1}$$

$$\eta^*_N \equiv \eta^* - \eta_e = n_N kT \sum_p \frac{\tau_{p,N}}{1 + i\omega\tau_{p,N}} \tag{2}$$

with q' an optical factor, n_N the number density of chains in solution, b^2 the mean-square distance between connected beads in a nonflowing solution, k the Boltzmann constant, T the absolute temperature, $\tau_{p,N}$ the relaxation time for the pth mode, $i = \sqrt{-1}$, and $\sum_p$ indicating a sum over all N normal modes. S_e and η_e are frequency-independent terms usually dominated by chain environment contributions. Historically they have been assumed to be identical with bulk solvent properties (S_s and η_s) or ϕS_s and $\phi\eta_s$ (where ϕ is the volume fraction of solvent); however, this has recently been shown to be incorrect, in general.[10-12] For the special case of an isorefractive homopolymer/solvent system, the optical factor is taken to be related to the index of refraction, n_s, of the solvent and the intrinsic optical anisotropy, $\alpha_1 - \alpha_2$, of the Kuhn statistical segment by

$$q' = \frac{4\pi}{45} \frac{(n_s^2 + 2)^2}{n_s} \frac{\alpha_1 - \alpha_2}{b^2} \tag{3}$$

Each relaxation time, $\tau_{p,N}$, is inversely proportional to $\lambda_{p,N}$, one of the N positive and nondegenerate eigenvalues of the real symmetric matrix $\mathbf{L}$.[6]

$$\tau_{p,N} = \frac{b^2\zeta}{6kT\lambda_{p,N}} \tag{4}$$

Polydisperse samples are modeled assuming that ζ, b^2, η_e, S_e, and q' are independent of chain size N and that N is proportional to the molecular weight M of the chain ($M = M_{sm}N$). There is ample experimental data,[13-15] including new data reported here, supporting such assumptions. In addition, the solutions are assumed to be sufficiently dilute that interchain interactions are negligible so that the solution properties can be represented by

$$S^* = \sum_N S^*_N + S_e \tag{5}$$

$$\eta^* = \sum_N \eta^*_N + \eta_e \tag{6}$$

with $\sum_N$ indicating a sum over all chain sizes. These expressions can be converted into reduced format in a manner similar to that used for monodisperse samples.[1] The reduced magnitude and angle for polydisperse samples are

$$\frac{[\eta_{M\Delta}]}{[\eta_{M\Delta o}]} = \frac{[S_{M\Delta}]}{[S_{M\Delta o}]} = \frac{\sum_N f[N](\Lambda_{1,N}^2 + (\omega\tau_{1,N}\lambda_{1,N})^2\Lambda_{2,N}^2)^{1/2}}{\sum_N f[N]\sum_p \lambda_{p,N}^{-1}} \tag{7}$$

$$[\Phi_\Delta] - [\Phi_{\Delta o}] = -([\Theta_\Delta] - [\Theta_{\Delta o}]) = +\tan^{-1}\left((\omega\tau_{1,N}\lambda_{1,N})\frac{\sum_N f[N]\Lambda_{2,N}}{\sum_N f[N]\Lambda_{1,N}}\right) \tag{8}$$

with

$$\Lambda_{1,N} = \sum_p \frac{\lambda_{p,N}^{-1}}{1 + (\omega\tau_{1,N})^2(\lambda_{1,N}/\lambda_{p,N})^2} \tag{9}$$

$$\Lambda_{2,N} = \sum_p \frac{\lambda_{p,N}^{-2}}{1 + (\omega\tau_{1,N})^2(\lambda_{1,N}/\lambda_{p,N})^2} \tag{10}$$

and $f[N]$ the fraction of chains of size N in the polydisperse sample, $\bar{N}$ the most probable chain size, and $\omega\tau_{1,\bar{N}}$ a reduced shearing frequency.

A. Computation of the Predicted Properties. Reduced dynamic properties for polydisperse samples are computed with eqs 7–10 using a table of Zimm eigenvalue spectra computed for the same degree of hydrodynamic interaction for every N up to 700. The eigenvalues are computed as reported previously[1] and are accurate to three or more significant figures. The degree of hydrodynamic interaction is specified by the parameter h^*.

$$h^* = \frac{\zeta}{\eta_e}\left(\frac{1}{12\pi^3 b^2}\right)^{1/2} \tag{11}$$

In this model h^* is independent of N since ζ, b^2, and η_e have been assumed to have no N dependence. This is expected to be a good assumption for data measured at or near Θ conditions. In better solvating conditions h^* is expected to show a very weak decrease with increasing chain size because the interbead dimensions, $b\langle r_{\nu\mu}^{-1}\rangle$, have not been corrected for excluded volume effects in the Zimm model. Recent computations[2] indicate this weak dependence should be insignificant until N reaches about 200 (molecular weights about 3×10^5 for polystyrene in Aroclor 1248) and small but observable for larger chains.

The distribution $f[N]$ of discrete chain sizes in solution is obtained from the molecular weight distribution, $f(M)$. Due to the discrete nature of the model, $f[N]$ is set equal to $f(M)$ whenever $M = M_{sm}N$ (N is a positive integer). The distribution is then truncated to reduce computational labor at low and high N when $f[N]$ is so small that it no longer affects the first three significant figures of the reduced magnitude or angle. Finally, the distribution is normalized such that $\sum_N f[N] = 1$. Of course the density of modes in distribution $f(M)$ exceeds that of distribution $f[N]$ by a factor of M_{sm}. This factor generally ranges between 20 and 50, and it follows that averaged properties do depend slightly on the choice of the distribution function. However, for most properties of interest here, the molecular weights (and number of modes per distribution function) are sufficiently high that there is little difference between properties averaged with $f[N]$ or $f(M)$.

B. Most Probable Distribution. The most probable molecular weight distribution[16] is predicted from condensation of a bifunctional monomer of type A–B when site A only reacts with site B, and the reactivity is independent of chain length. The idealized distribution depends on the monomer molecular weight, M_o, and the fraction, p_o, of functional groups that have reacted:

$$f(M) = (1 - p_o)p_o^{(M/M_o - 1)} \tag{12}$$

with $M/M_o = 1, 2, 3, \ldots, \infty$. The first three molecular weight averages of this distribution are $\bar{M}_z = M_o/(1 - p_o)$, $\bar{M}_w = M_o(1 + p_o)/(1 - p_o)$, and $\bar{M}_z = M_o(1 + 4p_o + p_o^2)/(1 - p_o^2)$; the polydispersity index is $\bar{M}_w/\bar{M}_n = + p_o$, and the most probable molecular weight is also M_o. As the condensation reaction tends toward completion, $p_o \to 1$ and $\bar{M}_w/\bar{M}_n \to 2$; this yields a level of polydispersity useful for illustrating typical polydispersity effects on dynamic properties.

Predictions of the reduced dynamic properties for one polydisperse sample and for three monodisperse samples are illustrated in Figure 1 for the free-draining limit ($h^* \to 0$) and $M_{sm} = 5000$ g/mol. The logarithm of the reduced magnitude, $\log([S_{M\Delta}]/[S_{M\Delta o}])$, and reduced angle, $-([\Theta_\Delta] - [\Theta_{\Delta o}])$, are both plotted as ordinates against the logarithm of the reduced angular shearing frequency, $\log(\omega\tau_{1,\bar{N}})$. The most probable chain size is $\bar{N} = 1$. The polydisperse sample has a most probable molecular weight distribution described by $M_o = 100$ g/mol and $p_o = 0.999$; the monodisperse samples are chosen to have molecular weights corresponding to the $\bar{M}_n$, $\bar{M}_w$, and $\bar{M}_z$ of the polydisperse sample. Only the properties of the polydisperse sample are unlabeled in the figure. Its reduced-angle curve is distinctive in that it gradually rises with increasing frequency. The usual features (lengthy plateau and sharp transition zones) of monodisperse samples are washed out, and hence polydispersity is expected to restrict characterization of long-chain structure in homopolymers via dynamic experiments. However, the washed-out features are advantageous in that they can be used to estimate $\bar{M}_n$ and $\bar{M}_z$ once calibration measurements are made with monodisperse samples to establish h^* and M_{sm} for the particular homopolymer/solvent system. $\bar{M}_z$ is estimated from the low-frequency portion of the reduced angle as it begins to deviate from 0°. This portion of the curve can be fit with predictions for *monodisperse samples*, and the product of the chain size parameter N arising from the fit and M_{sm} is a good estimate of $\bar{M}_z$. Likewise, $\bar{M}_n$ is estimated from the reduced angle curve at high frequency when its shape can again be described by predictions for monodisperse samples. The reduced magnitude of the polydisperse sample monotonically drops with increasing frequency; it is difficult to observe in the figure because at the lower (or higher) frequencies it almost superposes with the curve for a monodisperse sample computed for $M = \bar{M}_z$ (or $M = \bar{M}_w$). The latter result enables estimates of $\bar{M}_w$ after calibration factors h^* and M_{sm} are known.

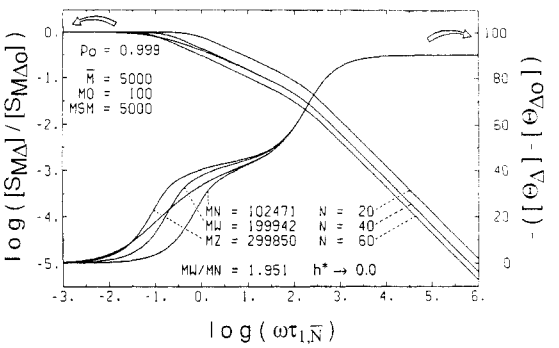

Figure 1. Predictions of reduced dynamic properties at the free-draining limit ($h^* \to 0.00$) for a polydisperse sample (most probable distribution: $p_o = 0.999$, $M_o = 100$ g/mol; $M_{sm} = 5000$; $\bar{M}_w/\bar{M}_n = 1.95$) and for three monodisperse samples having molecular weights coinciding with $\bar{M}_n$, $\bar{M}_w$, and $\bar{M}_z$ of the polydisperse sample.

Estimates of $\bar{M}_n$, $\bar{M}_w$, and $\bar{M}_z$ from the reduced magnitude and angle are not restricted to samples having a most probable molecular weight distribution. This empirical result has been found for all distributions investigated to date, and each molecular weight average is expected to be accurate to about 15% for samples with $\bar{M}_w$ exceeding about 2×10^5 g/mol. Attempts to derive these relations for an arbitrary distribution indicate that the molecular weight averages actually found only approximate values of $\bar{M}_n$, $\bar{M}_w$, and $\bar{M}_z$ and depend on the degree of hydrodynamic interaction. The effects of h^* on the molecular weight averages obtained are small; the magnitude of this effect can be seen by comparing the predictions in Figure 1 ($h^* \to 0$) to those in Figure 2 ($h^* = 0.25$) since the averaged properties are computed with the same molecular weight distribution.

C. Low Levels of Polydispersity. Here the effects

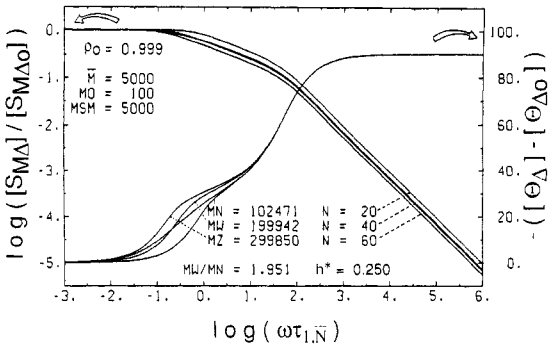

Figure 2. Predictions of reduced dynamic properties at the non-free-draining limit ($h^* = 0.25$) for a polydisperse sample (most probable distribution: $p_o = 0.999$, $M_o = 100$ g/mol; $M_{sm} = 5000$; $\bar{M}_w/\bar{M}_n = 1.95$) and for three monodisperse samples having molecular weights coinciding with $\bar{M}_n$, $\bar{M}_w$, and $\bar{M}_z$ of the polydisperse sample.

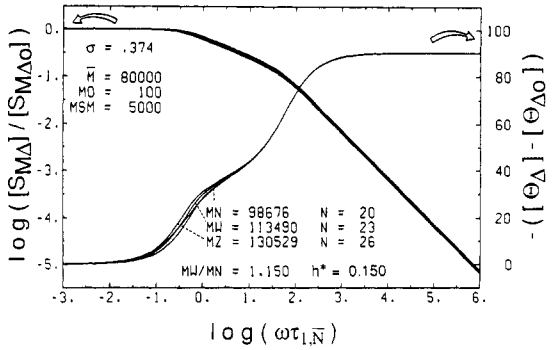

Figure 3. Predictions of reduced dynamic properties at $h^* = 0.15$ for a polydisperse sample (ZOL distribution: $\bar{M} = 80\,000$ g/mol, $\sigma = 0.374$; $M_{sm} = 5000$; $\bar{M}_w/\bar{M}_n = 1.15$) and for three monodisperse samples having molecular weights coinciding with $\bar{M}_n$, $\bar{M}_w$, and $\bar{M}_z$ of the polydisperse sample.

of polydispersity on the dynamic properties are investigated at levels ($\bar{M}_w/\bar{M}_n \simeq 1.15$) common to molecular weight standards. The dynamic properties of a sample with such a low level of polydispersity are expected to be indistinguishable regardless of the distribution function assumed to empirically approximate the molecular weight distribution. This has been substantiated in part from modeling predictions for six assumed functions, and so for convenience a zeroth-order logarithmic (ZOL) distribution[17] has been chosen. This two-parameter distribution is more commonly used in the analysis of particle sizes. While it works well for our particular application, caution is advised for more general uses since to our knowledge the ZOL distribution does not naturally arise from modeling any polymerization or fractionation procedure used to obtain molecular weight standards.

The ZOL distribution has a slight positive skew and allows a continuum of positive molecular weights. Its functional form is

$$f(M) = K \exp\left(-\frac{(\ln M/\bar{M})^2}{2\sigma^2}\right) \qquad (13)$$

with $K^{-1} = (2\pi)^{1/2}\sigma\bar{M}\exp(\sigma^2/2)$, $\bar{M}$ the most probable molecular weight, and σ the distribution breadth parameter. The first three molecular weight averages of this distribution are $\bar{M}_n = \bar{M}\exp(3\sigma^2/2)$, $\bar{M}_w = \bar{M}\exp(5\sigma^2/2)$, and $\bar{M}_z = \bar{M}\exp(7\sigma^2/2)$. The polydispersity index $\bar{M}_w/\bar{M}_n = \exp(\sigma^2)$ depends only on σ.

Polydispersity effects on reduced dynamic properties are illustrated in Figure 3 for a sample with a ZOL distribution ($\bar{M} = 80000$ g/mol, $\sigma = 0.374$; $\bar{M}_w/\bar{M}_n = 1.15$), $h^* = 0.15$, and $M_{sm} = 5000$ g/mol. As in the previous figures, curves of reduced magnitude and angle for the polydisperse sample are not labeled; the labeled curves are predictions for monodisperse samples. Inspection of the reduced-angle curves indicates that polydispersity, at such low levels, only affects the low-frequency transition zone; it decreases the steepness of the curve relative to that observed for monodisperse samples. Similar computations indicate that this effect should be experimentally observable in the reduced angle at polydispersity levels as low as $\bar{M}_w/\bar{M}_n = 1.08$ regardless of the degree of hydrodynamic interaction.

Table I
Polystyrene Samples

manufacturer	sample	$\bar{M}_w$, g/mol	$\bar{M}_w/\bar{M}_n$	$[\eta]$,[b] dL/g
Pressure Chemical	80314	9 000[a]	<1.06	0.12
Pressure Chemical	60917	53 700	<1.06	0.30
Pressure Chemical	4b	111 000	<1.06	0.43
Pressure Chemical	3b	390 000	<1.11	1.02
Pressure Chemical	6a	860 000	<1.15	1.66
Pressure Chemical	61124	1 800 000	<1.30	2.24
Dow Chemical	1683	250 000	2.5	0.73

[a] Only $\bar{M}_n$ is provided by the manufacturer. [b] Aroclor 1248, Lot KM 502; 25.0 °C.

III. Experimental Section

A. Materials. Seven samples of linear, atactic polystyrene have been investigated. Six samples have been purchased from the Pressure Chemical Co. as molecular weight standards with small polydispersities. The remaining sample is the broad molecular weight standard No. 1683 generously supplied by Dr. E. R. North of the Dow Chemical Co. Molecular weight characterizations provided by the manufacturers and our intrinsic viscosity results are summarized in Table I.

All samples were dissolved in Aroclor 1248, Lot KM 502, manufactured by the Monsanto Chemical Co. This chlorinated biphenyl solvent was selected because its viscosity has a strong dependence on temperature and because it is almost isorefractive with polystyrene. The latter property is expected to minimize form birefringence. Solutions were prepared by weight, and concentrations in grams per milliliter were computed at 25.00 °C, assuming additivity of volumes and using densities of 1.445 and 1.06 g/mL for Aroclor 1248 and polystyrene, respectively. The most concentrated solution for the narrow polydispersity standards was prepared by direct addition of polymer to solvent; the lower concentrations were made by diluting this stock solution. Solvation of the stock solutions was assisted with moderate heat (<60 °C) and occasional gentle stirring; they required 6–9 weeks depending on the molecular weight. The dilutions were treated with occasional gentle stirring and low heat (<40 °C) for at least 2 weeks before use.

The polydisperse standard was first transformed from clear extruded pellets to a fluffy white powder by freeze-drying a 1% solution in *p*-dioxane. The sample was dried for 2 days at pressures of about 100 μmHg; ^{1}H NMR analysis of the resulting powder dissolved in $CDCl_3$ indicated no detectable traces of *p*-dioxane. Each Aroclor 1248 solution was prepared by adding the polymer directly to the solvent. Solution was effected with low heat (<40 °C) and occasional gentle stirring over a period of 1 mo. The solutions were then filtered through 0.5-μm Millipore membranes to remove a fine white haze assumed to be insolubles arising from the pellet extruding process. After filtration they were subjected to more low heat and occasional stirring for another month.

The stock solution for the sample with the bimodal molecular weight distribution was made by combining portions of the solutions prepared for samples 4b and 6a. The ratio of polystyrene from sample 4b to that of 6a is 4.00 by weight, and the total concentration of polystyrene in the blend is 0.01648 g/mL. Mixing of this stock solution was assisted with occasional gentle stirring and low heat (<40 °C) for 2 weeks.

B. Oscillatory Flow Birefringence Measurements. The second-generation thin fluid layer OFB apparatus and measure-

ment procedures are described elsewhere.[7,8,18] The transducers of the apparatus are interfaced to a third-generation computerized data acquisition and processing system,[9-11] which substantially increases the effective frequency range and improves the sensitivity of the apparatus. All data were obtained using the 577.0-nm line of a Hg superpressure arc lamp and were acquired at five solution temperatures (+45.00, +25.00, +15.88, +2.81, and -1.42 °C). The temperature was controlled to ±0.01 °C with thermistors calibrated against an NBS-calibrated standard platinum resistance thermometer. Data at each temperature is obtained at about 20 shearing frequencies distributed in equal logarithmic steps between 0.25 and 1588 Hz. The uncertainties in the shearing or sampling frequencies are less than 1 part in 10^9. The precision of the OFB properties at each temperature, when expressed as $S^* - S_\infty' = S_{M\Delta} \exp(+i\Theta_\Delta)$, is usually ±0.4% for $S_{M\Delta}$ and ±0.3° for Θ_Δ; S_∞' ($\simeq S_e$) is the high-frequency, frequency-independent plateau observed in plots of S' versus frequency. The precision becomes poorer only when S^* is dominated by the contribution of the solvent (e.g., at very low molecular weight, at extremely dilute polymer concentrations, and/or at high shearing frequency).

Time-temperature superposition is used to empirically shift $S_{M\Delta}$ and Θ_Δ to reference temperature T_o = 25.00 °C at each concentration. Superpositions are done independently on the magnitude and on the angle. Though the shift factors a_T never differed by more than 2%, we report only values arising from the magnitude since the algorithm employed to obtain this a_T was slightly more precise. S_∞' is obtained at +2.81 and -1.42 °C from the analysis of $S' = \mathrm{Re}\{S^*\}$ measured for the solution at high frequency; it is identified as the limiting high-frequency slope of a plot of f^2S' versus f^2, where f denotes the shearing frequency in hertz. Examples of such plots are reported elsewhere.[12] At higher temperatures S_∞' must be estimated because a linear relationship no longer exists between f^2S' and f^2 at accessible f. The relationship

$$S_\infty'(T) = \phi(T)\, S_s(T) + (a_T/a_{T_1})[S_\infty'(T_1) - \phi(T_1)\, S_s(T_1)] \tag{14}$$

has been used to obtain $S_\infty'(T)$ at temperature T from data measured at T and T_1. Here, $\phi(T)$ is the volume fraction of solvent at temperature T, $S_s(T)$ is S^* measured for pure solvent at temperature T, and a_T is the time-temperature superposition shift factor arising from shifting data expressed as $S^* - \phi S_s = S_{M\phi} \exp(+i\Theta_\phi)$ from temperature T to reference temperature T_o. All estimates of S_∞' used T_1 = -1.42 °C, and values[10] of S_s for Aroclor 1248, Lot KM 502, measured at +45.00, +25.00, +15.88, +2.81, -1.42, -4.95, and -9.91 °C are (1.19 ± 0.1) × 10^{-10}, (6.07 ± 0.2) × 10^{-10}, (1.92 ± 0.1) × 10^{-9}, (2.34 ± 0.1) × 10^{-8}, (6.96 ± 0.3) × 10^{-8}, (2.00 ± 0.1) × 10^{-7}, and (1.10 ± 0.1) × 10^{-6} s, respectively.

Infinite-dilution properties, $[S_{M\Delta}]$ or $[\Theta_\Delta]$, are obtained independently from the extrapolations $\log [S_{M\Delta}] = \lim_{c\to 0} \log S_{M\Delta}/c$ and $[\Theta_\Delta] = \lim_{c\to 0} \Theta_\Delta$ (data at different concentrations measured at the same shearing frequency and temperature). Such extrapolations were linear in concentration c when $c[\eta] < 2$ and are of similar quality to those reported[19] previously. The dimensions of $[S_{M\Delta}]$ and $[\Theta_\Delta]$ used here are seconds·milliliters per gram and degrees, respectively.

IV. Results

A. Frequency Dependence of S^*_Δ. BSM computations are applicable to OFB data measured at finite concentration when the data is acquired at sufficiently dilute concentrations that interchain interaction effects are negligible. The effects of polymer concentration on the frequency dependence of S^*_Δ are shown in Figures 4–8 for samples with $\bar{M}_w$ of 9000, 111 000, 860 000, 1 800 000, and 250 000 g/mol, respectively. For clarity, a smooth curve is drawn through each set of 60–80 data points superposed to 25.00 °C. The product $c[\eta]$ ranges approximately between 0.5 and 4 for each of the four molecular weight standards with narrow polydispersity and between 0.4 and 1.8 for the polydisperse standard. Comparison of the two lowest concentrations of each figure indicates

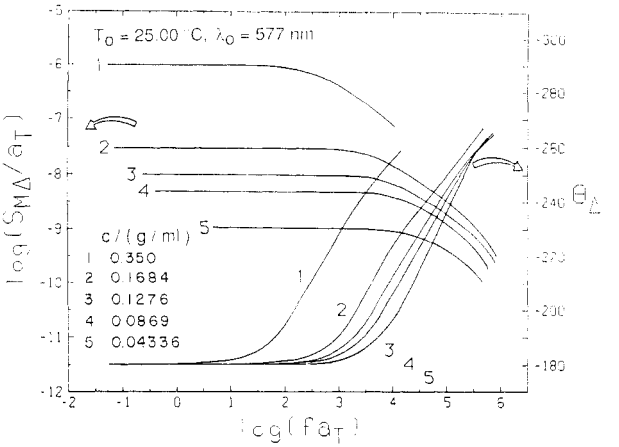

Figure 4. Measured concentration and frequency dependence of $S_{M\Delta}$ and Θ_Δ (λ_o = 577 nm, T_o = 25.00 °C) for polystyrene ($\bar{M}_w$ = 9000, $\bar{M}_w/\bar{M}_n$ = 1.06) in Aroclor 1248.

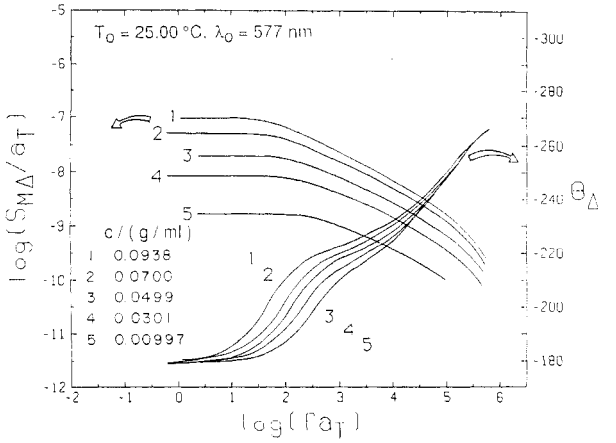

Figure 5. Measured concentration and frequency dependence of $S_{M\Delta}$ and Θ_Δ (λ_o = 577 nm, T_o = 25.00 °C) for polystyrene ($\bar{M}_w$ = 111 000, $\bar{M}_w/\bar{M}_n$ = 1.06) in Aroclor 1248.

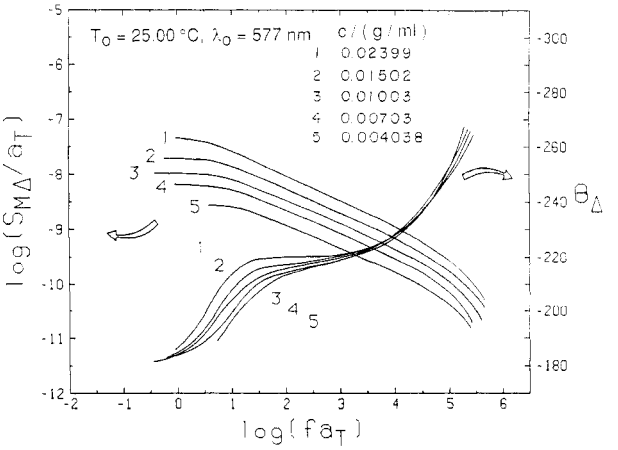

Figure 6. Measured concentration and frequency dependence of $S_{M\Delta}$ and Θ_Δ (λ_o = 577 nm, T_o = 25.00 °C) for polystyrene ($\bar{M}_w$ = 860 000, $\bar{M}_w/\bar{M}_n$ = 1.15) in Aroclor 1248.

that the properties still depend on c: as c decreases $S_{M\Delta}/a_T$ and Θ_Δ shift to higher fa_T and $S_{M\Delta}/a_T$ shifts down. However, the changes in the relative *shape* of the frequency dependence of $S_{M\Delta}/a_T$ or Θ_Δ are very small, and it is this shape that can be interpreted with the BSM. In section IV.B this argument is confirmed by showing that model parameters arising from fitting data measured at about $c[\eta]$ = 0.5 are the same as those arising from infinite-dilution properties. For those interested, the concentration dependence of the longest relaxation time τ_1

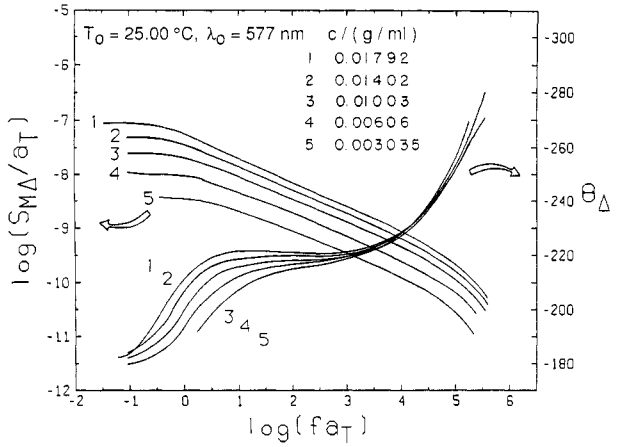

Figure 7. Measured concentration and frequency dependence of $S_{M\Delta}$ and Θ_Δ (λ_o = 577 nm, T_o = 25.00 °C) for polystyrene ($\bar{M}_w$ = 1 800 000, $\bar{M}_w/\bar{M}_n$ = 1.30) in Aroclor 1248.

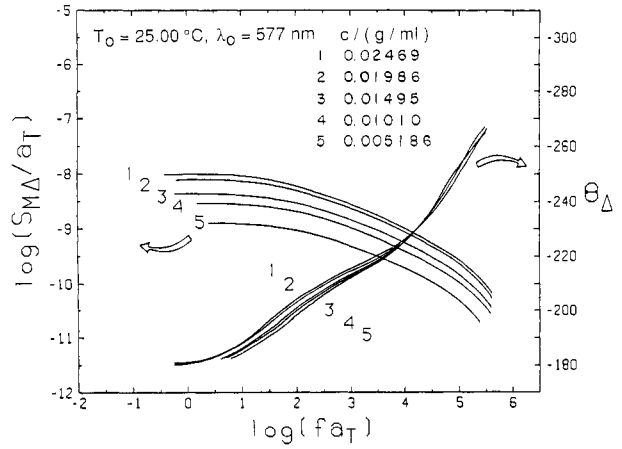

Figure 8. Measured concentration and frequency dependence of $S_{M\Delta}$ and Θ_Δ (λ_o = 577 nm, T_o = 25.00 °C) for polystyrene ($\bar{M}_w$ = 250 000, $\bar{M}_w/\bar{M}_n$ = 2.5) in Aroclor 1248.

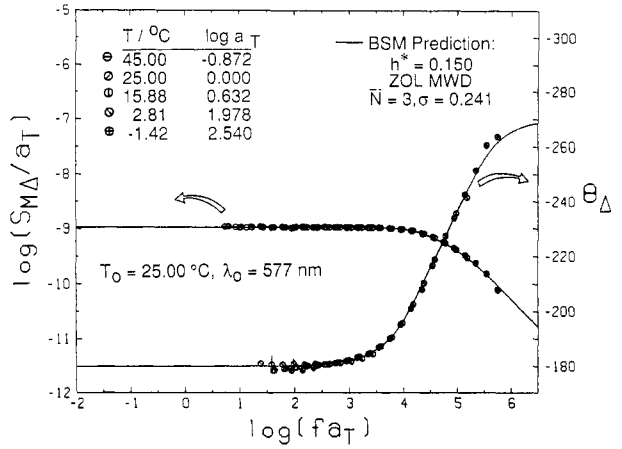

Figure 9. Measured frequency dependence of $S_{M\Delta}$ and Θ_Δ (λ_o = 577 nm, T_o = 25.00 °C) for polystyrene (c = 0.04336 g/mL, $\bar{M}_w$ = 9000 g/mol, $\bar{M}_w/\bar{M}_n$ = 1.06) in Aroclor 1248. Solid lines are BSM fits to data (circles) assuming a ZOL distribution with σ = 0.241, h^* = 0.15, and $\bar{N}$ = 3.

obtained for the narrow polydispersity standards with this data has been reported elsewhere.[20]

The frequency dependence of S^*_Δ measured for samples with narrow polydispersities and $\bar{M}_w$ of 9000, 53 700, 111 000, and 390 000 are shown in Figures 9–12. The product $c[\eta]$ values for these solutions were 0.50, 0.30, 0.43, and 0.46, respectively, and the data reported here for $\bar{M}_w$ of 9000 and 111 000 correspond to the lowest concentration data shown in Figures 4 and 5. This time the measured properties, reduced to 25.00 °C via time–temperature superposition, are displayed as discrete points. BSM fits to these properties are drawn as solid lines. The model predictions assume that the samples have a ZOL molecular weight distribution. The distribution breadth param-

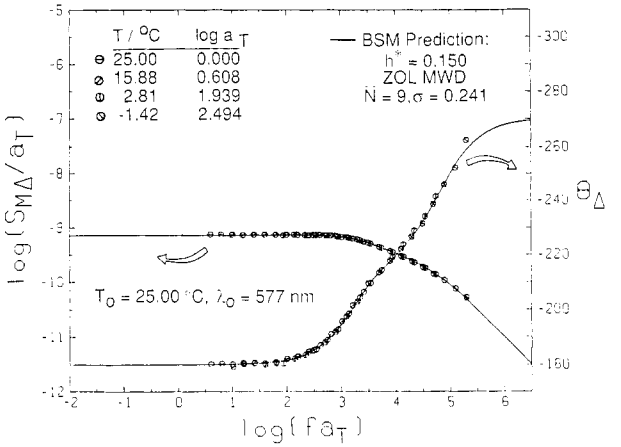

Figure 10. Measured frequency dependence of $S_{M\Delta}$ and Θ_Δ (λ_o = 577 nm, T_o = 25.00 °C) for polystyrene (c = 0.0099 g/mL, $\bar{M}_w$ = 53 700, $\bar{M}_w/\bar{M}_n$ = 1.06) in Aroclor 1248. Solid lines are BSM fits to data (circles) assuming a ZOL distribution with σ = 0.241, h^* = 0.15, and $\bar{N}$ = 9.

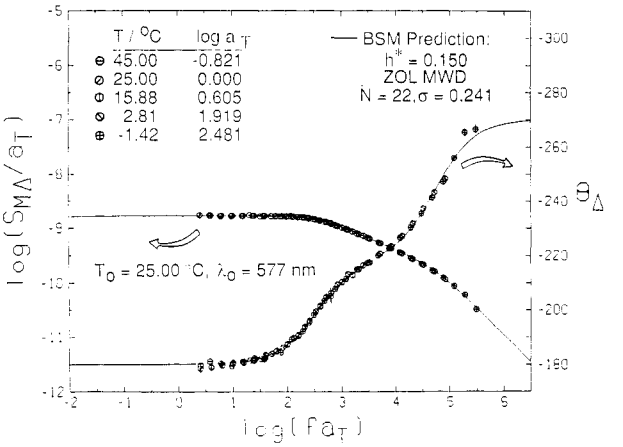

Figure 11. Measured frequency dependence of $S_{M\Delta}$ and Θ_Δ (λ_o = 577 nm, T_o = 25.00 °C) for polystyrene (c = 0.009 97 g/mL, $\bar{M}_w$ = 111 000, $\bar{M}_w/\bar{M}_n$ = 1.06) in Aroclor 1248. Solid lines are BSM fits to data (circles) assuming of ZOL distribution with σ = 0.241, h^* = 0.15, and $\bar{N}$ = 22.

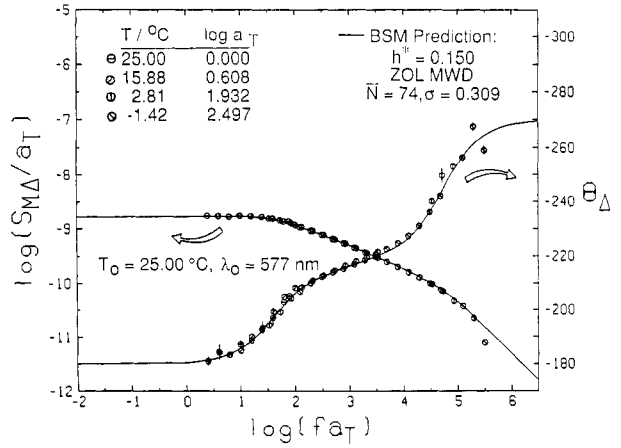

Figure 12. Measured frequency dependence of $S_{M\Delta}$ and Θ_Δ (λ_o = 577 nm, T_o = 25.00 °C) for polystyrene (c = 0.004 49 g/mL, $\bar{M}_w$ = 390 000, $\bar{M}_w/\bar{M}_n$ = 1.11) in Aroclor 1248. Solid lines are BSM fits to data (circles) assuming a ZOL distribution with σ = 0.309, h^* = 0.15, and $\bar{N}$ = 74.

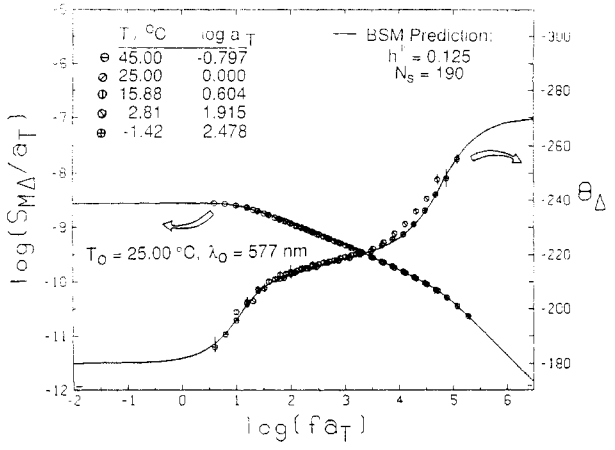

Figure 13. Measured frequency dependence of $S_{M\Delta}$ and Θ_Δ (λ_o = 577 nm, T_o = 25.00 °C) for polystyrene (c = 0.004 04 g/mL, $\bar{M}_w$ = 860 000, $\bar{M}_w/\bar{M}_n$ = 1.15) in Aroclor 1248. Solid lines are BSM fits to data (circles) ignoring sample polydispersity; h^* = 0.125 and N_s = 190.

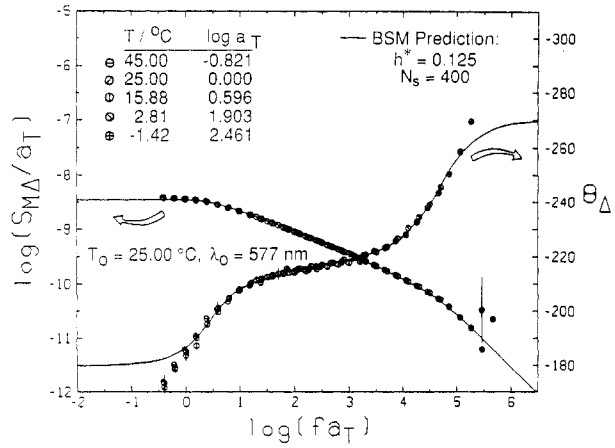

Figure 14. Measured frequency dependence of $S_{M\Delta}$ and Θ_Δ (λ_o = 577 nm, T_o = 25.00 °C) for polystyrene (c = 0.003 04 g/mL, $\bar{M}_w$ = 1 800 000, $\bar{M}_w/\bar{M}_n$ = 1.3) in Aroclor 1248. Solid lines are BSM fits to data (circles) ignoring sample polydispersity; h^* = 0.125 and N_s = 400.

eter, σ, was not varied to obtain this fit; it was simply set to the value obtained from the relation $\bar{M}_w/\bar{M}_n = \exp(\sigma^2)$, using the $\bar{M}_w/\bar{M}_n$ provided by the manufacturer. The value of h^* (or $\bar{N}$) used in each fit was ascertained from the height (or width) of the plateau in Θ_Δ. The frequency dependences of Θ_Δ and $S_{M\Delta}/a_T$ are fit quantitatively by the model; these fits are definitely superior to those obtained when polydispersity is ignored. The value of h^* is found to be essentially independent of molecular weight for these samples as is usually assumed for the model, and calculation of the Gaussian submolecule molecular weight, $M_{sm} = \bar{M}/\bar{N} = [\bar{M}_w \exp(-5\sigma^2/2)]/\bar{N}$, yields 2600 ± 1300, 5160 ± 500, 4400 ± 200, and 4150 ± 200 g/mol for samples with $\bar{M}_w$ of 9000, 53 700, 111 000, and 390 000, respectively. The average value (4200 g/mol) is 15% smaller than that estimated previously,[19] which was obtained ignoring sample polydispersity and assuming $S_e = \phi S_s$.

Data for the two higher molecular weight samples with narrow polydispersities are shown in Figures 13 and 14. The product $c[\eta]$ is 0.67 (or 0.68) for the sample with a $\bar{M}_w$ of 860 000 (or 1 800 000) g/mol. Sample polydispersity is *ignored* when this data is fit to model predictions because the larger chains in the distribution exceed the maximum size ($N \leq 700$) currently in our data base. Regardless, the fit to the data with the simple Zimm model is very good. Here, the value of hydrodynamic interac-

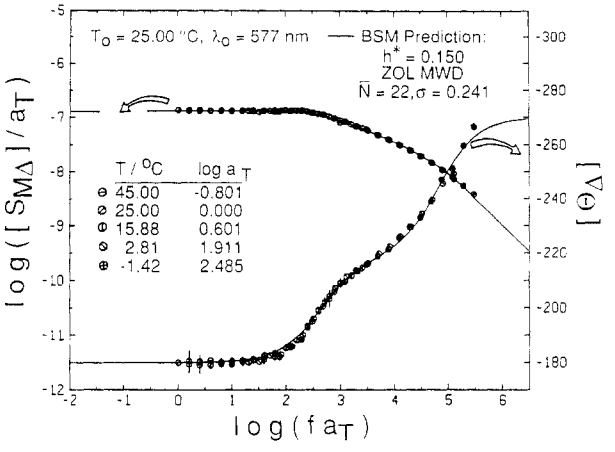

Figure 15. Measured frequency dependence of $[S_{M\Delta}]$ and $[\Theta_\Delta]$ (λ_o = 577 nm, T_o = 25.00 °C) for polystyrene ($\bar{M}_w$ = 111 000, $\bar{M}_w/\bar{M}_n$ = 1.06) in Aroclor 1248. Solid lines are BSM fits to data (circles) assuming a ZOL distribution with σ = 0.241, h^* = 0.15, and $\bar{N}$ = 22.

tion parameter, h^* (or number of springs N_s in the chain), is ascertained from the height (or width) of the plateau in Θ_Δ. The value of h^* (0.125) required for both fits is slightly lower than that (0.15) for the lower molecular weight samples. This drop is not caused by the neglect of sample polydispersity;[1] it may be due to excluded-volume effects expected[2] to be observable in the level of the plateau in Θ_Δ when N_s exceeds about 200. The Gaussian subchain molecular weight, $M_{sm} = \bar{M}_w/N_s$, estimated from these fits is 4500 ± 200 g/mol, which is in agreement with that found at lower molecular weight.

B. Frequency Dependence of $[S^*]_\Delta$. BSM predictions of dynamic properties are expected to be most applicable to measured properties after extrapolation to infinite dilution. Such extrapolations, when done properly, remove the effects of interchain interactions invariably present to some degree in all data measured at finite concentrations. An example of infinite-dilution properties is displayed in Figure 15. This sample has a narrow polydispersity and an $\bar{M}_w$ of 111 000 g/mol. The properties have been fit with the BSM (considering sample polydispersity) in the same manner as in section IV.A. The model parameters arising from such fits are the same as are observed at finite concentration (e.g., compare Figures 11 and 15). However, the fits to the infinite-dilution properties are not as good for samples with narrow polydispersities. The problem is most prevalent in Θ_Δ in the low-frequency transition zone (ca. log (fa_T) = 2). Here the data falls below the predictions of the model. Such a deviation is puzzling since our measurements are very precise in this region due to the high signal levels. It is not an excluded-volume effect,[2] and it vanishes when the sample polydispersity is higher (see below). Noting that the model predictions describe dilute-solution data so well, we suspect that our extrapolation method of obtaining infinite-dilution properties is inducing a small systematic error in regions where there is a sharp change in the properties with fa_T.

The infinite-dilution properties of the polydisperse molecular weight standard (Dow Chemical, No. 1683) are illustrated in Figure 16. The BSM predictions (solid lines) were computed *with no adjustable parameters*. The molecular weight distribution (provided by the manufacturer) used in eqs 7 and 8 was that measured for the standard via gel permeation chromatography (GPC), and h^* and M_{sm} for this homopolymer/solvent system are taken from the analysis of the narrow polydispersity standards. The model predictions clearly fit the data quan-

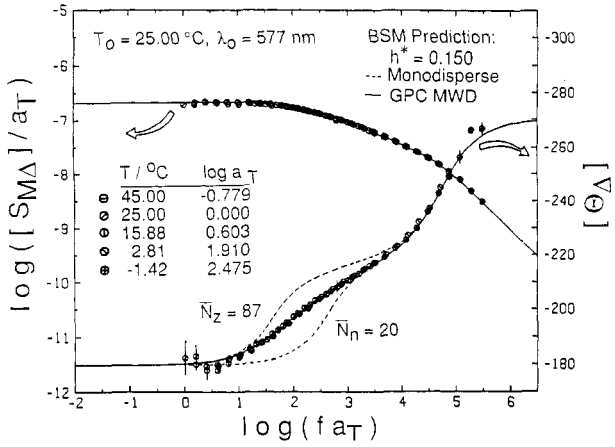

Figure 16. Measured frequency dependence of $[S_{M\Delta}]$ and $[\theta_\Delta]$ (λ_o = 577 nm, T_o = 25.00 °C) for polystyrene ($\bar{M}_w$ = 250 000, $\bar{M}_w/\bar{M}_n$ = 2.5) in Aroclor 1248. Solid lines are BSM predictions using the measured molecular weight distribution and values of h^* and M_{sm} ascertained from samples with narrow polydispersity.

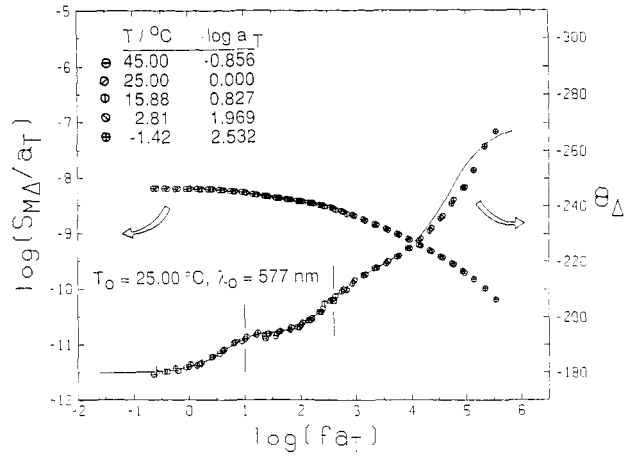

Figure 17. Measured frequency dependence of $S_{M\Delta}$ and Θ_Δ (λ_o = 577 nm, T_o = 25.00 °C) for a blend of polystyrene narrrow-polydispersity standard 4b ($\bar{M}_w$ = 111 000) and 6a ($\bar{M}_w$ = 860 000) in Aroclor 1248; 80% of the polystyrene concentration (0.016 48 g/mL) is sample 4b. The solid line is BSM fit to Θ_Δ assuming a two-component solution with h^* = 0.15 and 0.125 and N_s = 25 and 190 for 4b and 6a, respectively (τ_3(HMW) shifted to obtain fit; see text).

titatively. Model predictions ignoring polydispersity (broken lines) were successfully used to estimate the $\bar{M}_n$ and $\bar{M}_z$ from $[\Theta_\Delta]$; the precision of each estimate is about 10%.

C. Multimodal Molecular Weight Distributions. Application of this polydispersity model to multimodal distributions is its next important challenge. Measurements of OFB properties for blends of narrow-distribution polystyrene standards are currently in progress, but as yet they have been only completed for samples too concentrated to fairly assess the quantitative predictions of the model. Regardless, two important points pertaining to OFB properties of blends in the dilute and semidilute regime are now evident: (1) samples with multimodal molecular weight distributions can have multiple levels in the plateau region of angle Θ_Δ, and (2) the concentration dependence of the longest relaxation time τ_1 observed for the high molecular weight component in a blend may be substantially larger than is observed when it is the only component in solution. Both features have been observed in OFB data of bimodal and trimodal blends of narrow-distribution polystyrene standards;[10] data for a bimodal blend are illustrated and discussed in more detail below. The significance of the first point is that it again (see section II.B) underscores the need to assess sample polydispersity when using dynamic properties to interpret long-chain structure. This time, however, an ambiguity arises when a two-level plateau in Θ_Δ is observed, since such a feature is also observed for monodisperse samples of regular combs.[1,9,21] The origin of the second point is unknown; it is currently suspected to be an effect due to interaction between chains of different sizes although the concentration dependence of the relaxation times does not show the significant mode dependence usually observed.[20,22]

Both points are illustrated here with properties measured for a bimodal blend. The blend is composed of two of the narrow-distribution polystyrene standards used in sections IV.A and IV.B. The low molecular weight (LMW) component has a $\bar{M}_w$ of 111 000 g/mol; the high molecular weight (HMW) component has a $\bar{M}_w$ of 860 000 g/mol. The dilute solution OFB properties for the components are illustrated in Figures 11 and 13; the concentration dependence of τ_1 for the components has been reported elsewhere.[12,20,22] The properties of the blend are shown in Figure 17; here the circles denote the data measured at discrete frequencies. The two-level plateau in Θ_Δ is clearly visible and very similar to that for monodisperse samples of regular combs. The weight fraction of the LMW component is 0.800. The total polystyrene concentration is a 0.016 48 g/mL; the concentration of the LMW (or HMW) component is 0.013 18 g/mL (or 0.003 30 g/mL). Ignoring interactions between the two narrow-distribution components, one would expect at these concentrations that each component would be in its dilute regime since the product of the component concentration and its intrinsic viscosity (Table I) is below unity (0.57 or 0.55 for the LMW and HMW component, respectively). However, the data for the blend apparently is not in the dilute regime since extrapolation curves required to obtain infinite-dilution properties are nonlinear (combining this data with data[10] measured at higher concentrations). Not surprisingly, attempts to fit this data with no adjustable parameters as done in section IV.B[23] were poor since the polydispersity model ignores all types of interchain interaction. However, the model successfully predicts the observed two-level plateau in angle Θ_Δ.

Values of the longest relaxation times for the LMW or HMW components in the bimodal blend are 3.9×10^{-4} and 1.59×10^{-2} s, respectively. These values were ascertained by fitting the blend data with the polydispersity model again but this time multiplying all the relaxation times of the HMW component by a factor exceeding unity before using eqs 7 and 8. This artificially shifts the plateau of Θ_Δ for the HMW component to lower frequencies as is experimentally observed. (Shifting all relaxation times is unrealistic since there is ample experimental data indicating that the shortest relaxation time of both components is the same. Use of this type of shift is expected to cause the computed properties to deviate from those measured at high frequency as is observed. Currently, there are no theoretical predictions for the concentration dependence of the τ_1 values for blend solutions.) The best fit to the blend properties is illustrated with a solid line in Figure 17. The fit is surprisingly very good for all but the highest frequencies and hence is expected to give reliable estimates of τ_1 for both components. It also suggests that for blends in this concentration regime there is little evidence for a mode-dependent shift in the relaxation times.

The ratio of $(\tau_1)_{HMW}/(\tau_1)_{LMW}$ observed for the blend is 41. A much lower ratio is obtained when infinite-dilution τ_1 values are used for the components. Landry[12,20] determined τ_1° for each component (before blending) to be 2.70×10^{-4} and 6.84×10^{-3} s for the LMW and HMW component, respectively. Hence, the infinite-dilution ratio $(\tau_1^\circ)_{HMW}/(\tau_1^\circ)_{LMW}$ is 25 and is in very good agreement with a ratio of 27 from BSM predictions. Thus, the polymer concentration does have a substantial effect on the τ_1 values of blends. In addition, this concentration effect on τ_1 for blends is different than that[12,20] found when only one polymer component is in solution. For example, $(\tau_1/\tau_1^\circ)_{HMW}$ is 2.33 for the blend, but the ratio would be expected to only be 1.50 if only the HMW sample was in solution at a concentration of 0.003 30 g/mL. Likewise, $(\tau_1/\tau_1^\circ)_{LMW}$ is 1.44 for the blend but was expected to be 1.39. In summary, the τ_1 value's shift to longer times in the blends is more than expected when only one component is in solution, the τ_1 of the HMW component shifts much more than that of the LMW component in the blend, and the long-time portion of the relaxation time spectra of the two components appears to shift uniformly.

V. Conclusions

The effects of sample polydispersity on the frequency dependence of S^*_Δ can be modeled quantitatively for atactic samples of polystyrene dissolved in Aroclor 1248. At low levels of polydispersity the effects are only observed in the low-frequency transition zone; at higher levels the effects are observed at most frequencies. Estimates of various molecular weight averages from S^*_Δ data are possible after calibration with monodisperse standards. The molecular weight of a Gaussian submolecule for polystyrene dissolved in Aroclor 1248 at 25.00 °C is 4200 ± 500 g/mol. This result is independent of molecular weight for all samples studied. The hydrodynamic interaction parameter, h^*, is 0.15 for samples with $\bar{M}_w \leq 390\,000$ g/mol; h^* drops to 0.125 for samples with $860\,000 \leq \bar{M}_w \leq 1\,800\,000$ g/mol. A small decrease in h^* with molecular weight is expected from excluded-volume considerations. The dynamic properties of a sample of linear chains with a bimodal molecular weight distribution can be similar to those of a monodisperse sample of regular combs. This result underscores the need to independently assess sample polydispersity when using dynamic properties to interpret long-chain structure. Finally, the concentration dependence of the τ_1 for the high molecular weight component of the blend solution differs substantially from that observed before blending.

Acknowledgment. We thank Dr. Edwin R. North of the Dow Chemical Co. for graciously supplying the Dow No. 1683 polystyrene standard and its molecular weight distribution, B. LeBlanc for confirming the absence of *p*-dioxane in the freeze-dried Dow standard with a ^{1}H NMR experiment, D. Eisert for measuring the intrinsic viscosity of the Dow standard in Aroclor 1248, and Dr. T. M. Stokich for advice and unrestricted access to his unpublished work on measuring and/or estimating η_∞', which we applied to obtain S_∞'. This work was supported by the National Science Foundation Polymers Program through Grants DMR-8303207 and DMR-8800641.

References and Notes

(1) Sammler, R. L.; Schrag, J. L. *Macromolecules* **1988**, *21*, 3273.
(2) Sammler, R. L.; Schrag, J. L. *Macromolecules* **1989**, *22*, 3435.
(3) Lovell, S. E.; Ferry, J. D. *J. Phys. Chem.* **1961**, *65*, 2274.
(4) Zimm, B. H. *J. Chem. Phys.* **1956**, *24*, 269.
(5) Lodge, A. S.; Wu, Y.-J. *Rheol. Acta* **1971**, *10*, 539.
(6) Sammler, R. L.; Schrag, J. L. *Macromolecules* **1988**, *21*, 1132.
(7) Miller, J. W.; Schrag, J. L. *Macromolecules* **1975**, *8*, 361.
(8) Miller, J. W. Ph.D. Thesis, University of Wisconsin—Madison, 1979.
(9) Dibbs, M. G. Ph.D. Thesis, University of Wisconsin—Madison, 1983.
(10) Sammler, R. L. Ph.D. Thesis, University of Wisconsin—Madison, 1985.
(11) Stokich, T. M. Ph.D. Thesis, University of Wisconsin—Madison, 1988.
(12) Landry, C. J. T. Ph.D. Thesis, University of Wisconsin—Madison, 1985.
(13) Thurston, G. B.; Schrag, J. L. *J. Chem. Phys.* **1966**, *45*, 3373.
(14) Thurston, G. B. *J. Chem. Phys.* **1967**, *47*, 3582.
(15) Merchak, P. A. Ph.D. Thesis, University of Wisconsin—Madison, 1987.
(16) Flory, P. J. *Principles of Polymer Chemistry*; Cornell University Press: Ithaca NY, 1953; Chapter 8.
(17) Espensheid, W. F.; Kerker, M.; Matijevic, E. *J. Polym. Sci., Polym. Phys. Ed.* **1964**, *68*, 3093.
(18) Thurston, G. B.; Schrag, J. L. *Trans. Soc. Rheol.* **1962**, *6*, 325.
(19) Lodge, T. P.; Miller, J. W.; Schrag, J. L. *J. Polym. Sci., Polym. Phys. Ed.* **1982**, *20*, 1409.
(20) Martel, C. J. T.; Lodge, T. P.; Dibbs, M. G.; Stokich, T. M.; Sammler, R. L.; Carriere, C. J.; Schrag, J. L. *Faraday Symp. Chem. Soc.* **1983**, No. 18, 173.
(21) Peterson, P. S. MS Thesis, University of Wisconsin—Madison, 1985.
(22) Lodge, T. P.; Schrag, J. L. *Macromolecules* **1982**, *15*, 1376.
(23) A slightly simpler polydispersity calculation was employed here since the HMW sample contained chain sizes exceeding the limit of our data base ($N_s \leq 700$). The molecular weight distribution was approximated by a sum of just two molecular weight components. The properties of the LMW (or HMW) narrow-distribution component in the blend were modeled with parameters for isolated bead–spring chains with $N_s = 25$ and $h^* = 0.15$ (or $N_s = 190$ and $h^* = 0.125$) as ascertained in section IV.A before blending. Ignoring the narrow polydispersity of the standard only causes a modest degradation of the BSM fit to measured properties; for example, see Figures 13 and 4.